

Azobenzene-Containing Monolayer with Photoswitchable Wettability

N. Delorme,^{†,‡} J.-F. Bardeau,^{*,†} A. Bulou,[†] and F. Poncin-Epaillard^{*,‡}

Laboratoire de Physique de l'Etat Condensé (CNRS, UMR 6087) and Laboratoire Polymères, Colloïdes et Interfaces (CNRS, UMR 6120), Université du Maine, Avenue O. Messiaen, 72085 Le Mans Cedex 09, France

Received June 8, 2005. In Final Form: September 26, 2005

A compact monolayer containing azobenzene has been prepared on silicon substrates. The elaboration route consisted of covalent grafting of freshly synthesized azobenzene moieties onto an isocyanate-functionalized self-assembled monolayer (SAM). The highly packed and ordered isocyanate-functionalized SAM and the azobenzene-functionalized SAM were monitored and characterized by contact angle measurements and X-ray reflectivity (XR). Photoswitching of the wettability of the film induced by the reversible cis–trans isomerization of the azobenzene chromophores is experimentally shown from water and olive oil contact angle measurements.

Introduction

Two-dimensional nanostructures with chemical functionalities and physical properties based on the formation of highly ordered functionalized self-assembled monolayers (SAMs) have attracted increasing interest because of the great potential that such molecular architectures offer for chemical, biological, and medical applications.¹ More recently, specific research on microfluidics has been focused on fluid–surface interactions in microchannels based on surface tension or on special geometrical designs of wetting patterns.^{2,3} The field of microfluidics holds a lot of promise. The design of the microfluidics hardware differs from that of macroscale hardware. It is generally not possible to scale down conventional devices and then expect them to work in microfluidics applications. Hence, new ways have to be identified to manipulate small amounts of fluid. Thus, new functionalized solid surfaces whose wettability can be controlled by an external stimulus (radiation, electric field, etc.) have emerged.^{4,5}

Azobenzene derivatives are typical compounds adapted to prepare such a surface. Indeed, because these chromophores undergo photon-driven reversible cis–trans isomerization, they have been widely studied for potential applications in specific areas such as liquid crystal alignment,^{6,7} electrooptics,⁸ and information storage.⁹

It is well known that the physical and chemical properties of the two isomers are different¹⁰ and that

photoisomerization can induce changes in the dipole moment.¹¹ Therefore, the use of azobenzene molecules has received significant experimental and theoretical attention. However, the origins of the wettability variation are still obscure. Several mechanisms have been proposed in the literature: changes in the orientation of the functional units,¹² roughness introduced by illumination,¹³ and changes in the dipole moment.^{14–16}

In the same way, the influence of chromophore density on the wettability variation remains unclear. It has been reported that the density of the chromophore monolayer should be limited in order to allow the isomerization.^{4,16,17} However, Hamelmann et al. have recently shown the ability to elaborating a dense azobenzene monolayer showing a large variation of wettability.¹⁸

Self-assembled monolayer (SAM) depositions are among the most attractive for controlling molecular structure at the surface.¹ The preparation of SAMs containing azobenzene moieties onto silicon surfaces has already been described with two different synthesis methods.^{4,19–23} The

* To whom correspondence should be addressed. E-mail: jean-francois.bardeau@univ-lemans.fr; fabienne.poncin-epaillard@univ-lemans.fr.

[†] Laboratoire de Physique de l'Etat Condensé (CNRS, UMR 6087).

[‡] Laboratoire Polymères, Colloïdes et Interfaces (CNRS, UMR 6120).

(1) Ulman, A. *Chem. Rev.* **1996**, *96*, 1533–1554.

(2) Zhao, B.; Moore, J. S.; Beebe, D. J. *Science* **2001**, *291*, 1023–1026.

(3) Feng, Y.; Zhou, Z.; Ye, X.; Xiong, J. *Sens. Actuators, A* **2003**, *108*, 138–143.

(4) Ichimura, K.; Oh, S.-K.; Nakagawa, M. *Science* **2000**, *288*, 1624–1626.

(5) Cooper, C. G. F.; MacDonald, J. C.; Soto, E.; McGimpsey, W. G. *J. Am. Chem. Soc.* **2004**, *126*, 1032–1033.

(6) Ichimura, K. *Mol. Cryst. Liq. Cryst.* **1997**, *298*, 221–226.

(7) Manaka, T.; Taguchi, D.; Nakamura, D.; Higa, H.; Iwamoto, M. *Colloids Surf., A* **2005**, *257–258*, 319–323.

(8) Willner, I.; Pardo-Yissar, V.; Katz, E.; Ranjit, K. T. *J. Electroanal. Chem.* **2001**, *497*, 172–177.

(9) Chaput, F.; Riehl, D.; Lévy, Y.; Boilot, J.-P. *Chem. Mater.* **1993**, *5*, 589–591.

(10) Rau, H. Photoisomerization of Azobenzenes. In *Photochemistry and Photophysics*; Rabek, J. F., Ed.; CRC Press: Boca Raton, FL, 1990; Vol. 1, Chapter 2, pp 119–143.

(11) Stiller, B.; Knochenhauer, G.; Markava, E.; Gustina, D.; Muzikante, I.; Karageorgiev, P.; Brehmer, L. *Mater. Sci. Eng., C* **1999**, *8–9*, 385–359.

(12) Möller, G.; Harke, M.; Motschmann, H.; Prescher, D. *Langmuir* **1998**, *14*, 4955–4957.

(13) Ishihara, K.; Okazaki, A.; Negishi, N.; Shinohara, I.; Kataoka, K.; Sakurai, Y. *J. Appl. Polym. Sci.* **1982**, *27*, 239.

(14) Sarkar, N.; Bhattacharjee, S.; Sivaram, S. *Langmuir* **1997**, *13*, 4142–4149.

(15) Stiller, B.; Karageorgiev, P.; Jungling, T.; Prescher, D.; Zetzsch, T.; Dietel, R.; Knochenhauer, G.; Brehmer, L. *Mol. Cryst. Liq. Cryst.* **2001**, *355*, 401–405.

(16) Raduge, C.; Papastavrou, G.; Kurth, D. G.; Motschmann, H. *Eur. Phys. J. E* **2003**, *10*, 103–114.

(17) Aoki, K.; Seki, T.; Suzuki, Y.; Tamaki, T.; Hosoki, A.; Ichimura, K. *Langmuir* **1992**, *8*, 1007–1013.

(18) Hamelmann, F.; Heinzmann, U.; Siemeling, U.; Bretthauer, F.; Vor der Brüggen, J. *Appl. Surf. Sci.* **2004**, *222*, 1–5.

(19) Ichimura, K.; Suzuki, Y.; Seki, T.; Hosoki, A.; Aoki, K. *Langmuir* **1988**, *4*, 1214–1216.

(20) Siewierski, L. M.; Brittain, W. J.; Petrash, S.; Foster, M. D. *Langmuir* **1996**, *12*, 5838–5844.

(21) Sekkat, Z.; Wood, J.; Geerts, Y.; Knoll, W. *Langmuir* **1995**, *11*, 2856–2859.

(22) Sekkat, Z.; Wood, J.; Geerts, Y.; Knoll, W. *Langmuir* **1996**, *12*, 2976–2980.

(23) Mouanda, B.; Viel, P.; Blanche, C. *Thin Solid Films* **1998**, *323*, 42–52.

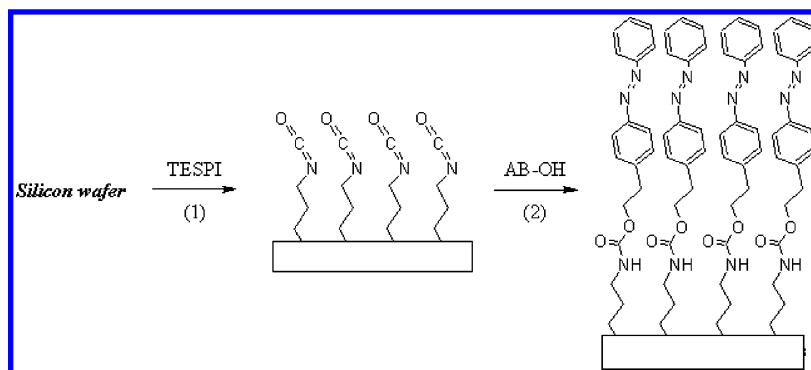


Figure 1. Schematic outline of the procedure used to elucidate the compact azobenzene-containing monolayer by grafting chromophores onto the SAM-modified Si substrate.

first method consists of the chemisorption of triethoxysilane containing an azobenzene moiety (azo-silane).^{19–23} However, this process did not allow a dense azobenzene monolayer to form, probably because of the difficulties with purification during the synthesis of the azo-silane.²² The second synthesis route consists of forming a dense functionalized self-assembled monolayer on which, in a second step, azobenzene moieties are grafted.^{4,18,20} Siewierski et al. have shown that this method gives rise to a higher density for the monolayer containing azobenzene moieties.²⁰

In this article, we describe the preparation of a dense monolayer containing azobenzene derivatives onto a silicon surface such that the wettability can be controlled by light. Our approach consists of two key steps as shown in Figure 1. First, an alkylsilane SAM containing an isocyanate function (TESPI) is formed on a silicon substrate, and subsequently an azobenzene derivative (AB-OH) is covalently grafted on it. Such an approach allows accurate step-by-step control of the processes by contact angle measurements, AFM, and X-ray reflectivity analysis of the architectures. The photodependent wettability properties of such systems were then evidenced by alternate exposure to UV ($\lambda = 325$ nm) and visible ($\lambda = 442$ nm) radiation of a HeCd laser.

Experimental Section

Synthesis of 4-(Phenylazo)phenethyl Alcohol (AB-OH).²⁴ Aminophenethyl alcohol (14.8 g) and nitrosobenzene (9.8 g) were dissolved in absolute ethanol (100 mL). The mixture was stirred for 15 min, and glacial acetic acid (10 mL) was added slowly. The mixture was then heated to reflux over the course of 2 h. After cooling to room temperature, the solution was poured into distilled water (1 L). The precipitate was filtered and air dried. The solid was recrystallized from an ethanol/water mixture (3/2 by volume). Yield: 86%. ¹H NMR (CDCl₃): δ 1.25 ppm (–OH), 2.95 ppm (Ar–CH₂–), 3.92 ppm (–O–CH₂–), 7.27 ppm (aromatic, ortho to –CH₂–), 7.49 ppm (aromatic, meta and para to –N=N–), 7.92 ppm (aromatic, ortho to –N=N–).

Substrates. Single-sized polished silicon wafers from Siltronic (orientation {100}) were cleaned in pure ethanol (Aldrich) in an ultrasonic bath for 5 min, followed by immersion in a piranha solution (70% H₂SO₄/30% H₂O₂) at 100 °C for 5 min. Afterward, the wafers were rinsed with deionized water, dried in a nitrogen stream, and placed into the chamber of a UV–ozone cleaner (UVO cleaner, Jelight Company Inc.) for 10 min. The silicon wafers were immediately used in order to prevent surface contamination.

Film Preparation. Self-assembled monolayers of alkylsiloxanes were prepared from solutions of 3-isocyanatopropyltriethoxysilane (TESPI-Fluka) in bicyclohexyl (Fluka, purity

$\geq 99\%$). Experiments were performed in a Teflon beaker using a TESPI concentration of 4×10^{-4} mol·L^{–1}.

The grafting reaction between 4-(phenylazo)phenethyl alcohol (AB-OH) and the isocyanate-functionalized SAM was realized by placing in a three-necked flask purged with argon the silanized wafer in a solution containing 10 mL of anhydrous dioxane (Aldrich), 5×10^{-3} g of AB-OH, 0.2 mL of triethylamine (Aldrich, 99.5%), and one crystal of dibutyltin bis(2-ethylhexanoate) as previously reported.²³ The resulting mixture was heated to reflux for 15 h under an argon atmosphere. After immersion, the wafers were rinsed in toluene in an ultrasonic bath for 1 min to remove nongrafted molecules.

Characterization. Water contact angle measurements were performed using a Ramé-Hart Inc. goniometer. Three drops of deionized water (3 μ L) were used to measure the wettability of the surface.

AFM measurements were performed with a Nanoscope III Multimode SPM from Veeco in tapping mode under ambient conditions. The surface roughness was evaluated by the root-mean square (rms), which can be expressed as $\text{rms} = [\sum_i (Z_i - Z_{\text{av}})^2/n]^{1/2}$ where Z_i is the height at point i , Z_{av} is the average of Z , and n is the number of data points. The reported rms values were calculated using WSxM 4.0 software developed by Nanotec Electronica S. L.

X-ray reflectivity curves were obtained with a Philips X'Pert MPD in a parallel beam optics configuration. The X-ray wavelength source was 1.54 Å (K α -ray of Cu). Refinement of the normalized Fresnel reflectivity on the basis of the matrix method²⁵ (preferred to the Born approximation²⁶) gives the electron thickness, roughness, and electron densities of the different stacks (molecules and molecular sequences). In these treatments, the silicon substrate is supposed to have an infinite thickness, and its electron density is fixed ($0.710 \text{ e}^{-}\cdot\text{\AA}^{-3}$);²⁷ similarly, the electron density of the oxide layer, always present on silicon surface²⁸ was fixed at $0.670 \text{ e}^{-}\cdot\text{\AA}^{-3}$.²⁹

Photoisomerization. Photoisomerization investigations were carried out by exposing the sample surfaces to a He–Cd laser beam. The two available wavelengths at 325 nm ($P = 0.33 \text{ W}\cdot\text{cm}^{-2}$) and 442 nm ($P = 0.86 \text{ W}\cdot\text{cm}^{-2}$) allow us to modify the conformation of the azobenzene molecules and verify the wettability modifications related to irradiation contact.

Results and Discussion

Isocyanate-Functionalized SAM. Figure 2 shows the evolution of the water contact angle as a function of the silanization time. At the beginning, the water contact angle was close to 0°, indicating that the cleaning process used

(25) Baptiste, A.; Gibaud, A.; Bardeau, J. F.; Wen, K.; Maoz, R.; Sagiv, J.; Ocko, B. M. *Langmuir* **2002**, *18*, 3916–3922.

(26) *X-ray and Neutron Reflectivity: Principles and Applications*; Gibaud, A.; Daillant, J., Eds.; Springer: Paris, 1999.

(27) Tidswell, I. M.; Ocko, B. M.; Pershan, P. S.; Wasserman, S. R.; Whitesides, G. M. *Phys. Rev. B* **1990**, *41*, 1111.

(28) Sokrates, K.; Pantelides, T. *The Physics of SiO₂ and Its Interfaces*; Pergamon: New York, 1978.

(29) Wasserman, S. R.; Whitesides, G. M.; Tidswell, I. M.; Ocko, B. M.; Pershan, P. S.; Axe, J. D. *J. Am. Chem. Soc.* **1989**, *111*, 5852–5861.

(24) Natansohn, A.; Rochon, P.; Ho, M.-S.; Barrett, C. *Macromolecules* **1995**, *28*, 4179.

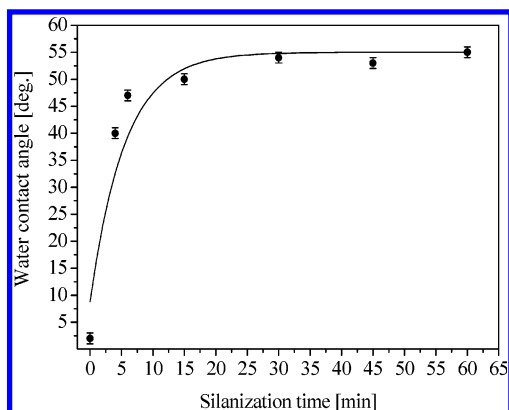


Figure 2. Water contact angle as a function of the TESPI silanization time.

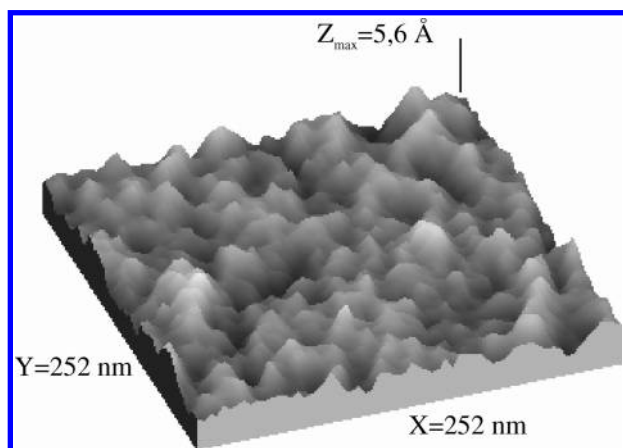


Figure 3. AFM topography image (252 nm × 252 nm) of the isocyanate-functionalized SAM ($t = 45$ min).

in our experiment allows a total decontamination and the formation of silanol groups on the wafer surface. The water contact angle value rapidly increases with the silanization time until a plateau value ($53^\circ \pm 2$) after about 30 min, which may correspond to the surface saturation with isocyanate groups.

The topographic characteristics of the surface of the film were controlled by AFM measurements. The AFM topography image (252 nm × 252 nm) illustrated in Figure 3 proves that the surface of the sample is very smooth once the water contact angle plateau is reached. This is quantitatively shown by the weakness of the rms roughness equal to 0.07 nm. Furthermore, we did not observe defects at larger scale ($1 \mu\text{m} \times 1 \mu\text{m}$), which confirms that the film can be considered to be homogeneous.

The X-ray reflectivity curves (Figure 4) clearly show the emergence of oscillations, proving the development of uniform layers with a shift of the first minimum toward lower Q_z indicating a progressive increase in the SAM thickness.²⁹ Moreover, the relative decrease in the intensity of the minimum can be straightforwardly assigned to the progressive increase in the molecular packing. No change is observed for reaction times greater than 45 min. The characteristics of such a film deduced from the refinement of the reflectivity curve are given in Table 1 (model 1). The different components of the stacking are shown in Figure 5, each one being characterized by its electron density, thickness, and roughness. In addition to the silicon substrate and the silicon oxide layer, the architecture consists of a transition layer, the alkyl layer, and the isocyanate layer. The former includes the complex interface between the silicon oxide and the alkyl chain of

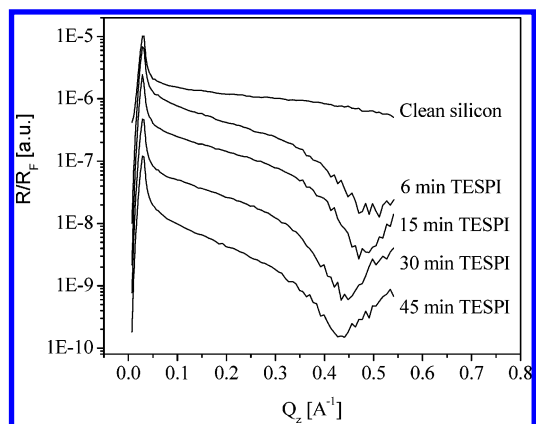


Figure 4. Evolution of the Fresnel-normalized X-ray reflectivity curves of clean silicon and the TESPI SAM as a function of silanization time.

Table 1. Parameters Obtained from the Fit of the X-ray Reflectivity Curve of the Isocyanate-Functionalized SAM (Model 1) and Grafted with ABOH (Model 2)

		ρ [e ⁻ ·Å ⁻³]	roughness [Å]	thickness [Å]
model 2	ABOH layer	0.380	1.4	13.7
model 1	isocyanate layer	0.411 ^a	0.9	2.5 ^a
	alkyl layer	0.312 ^a	2.5 ^a	3.8 ^a
	transition layer	0.558 ^a	1.6 ^a	2.2 ^a
	oxide layer	0.670 ^a	4.1 ^a	11.9 ^a
	substrate	0.710 ^a	0.1 ^a	

^a Parameters maintained fixed during the fit.

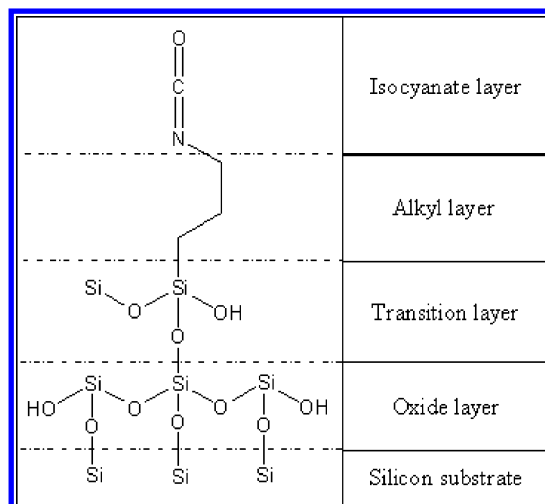


Figure 5. Five-layer model used for the analysis of the TESPI self-assembled monolayer reflectivity curve.

the TESPI molecules.^{25,29–31} TESPI molecules are divided into two layers, the alkyl chain (i.e., three $-\text{CH}_2-$ groups) and the isocyanate “head”.

The Q_z value of the first minimum at 0.435 \AA^{-1} (denoted $Q_{z\text{min}}$) is a good indicator of the quality of the SAM, yielding to an approximate total film thickness of 7 Å following the relation ($L = \pi/Q_{z\text{min}}$).²⁹ The total film thickness calculated from $Q_{z\text{min}}$ is in good agreement with the predicted length of 7.3 Å corresponding to fully extended TESPI molecules in an all-trans conformation. Therefore, taking into account this result, the thickness of the alkyl layer was kept at $L = 1.27 \times 3 = 3.8 \text{ \AA}$, corresponding to an all-trans

(30) Wasserman, S. R.; Tao, Y.-T.; Whitesides, G. M. *Langmuir* **1989**, 5, 1074–1087.

(31) Richter, A. G.; Yu, C.-J.; Datta, A.; Kmetko, J.; Dutta, P. *Phys. Rev. E* **2000**, 61, 607.

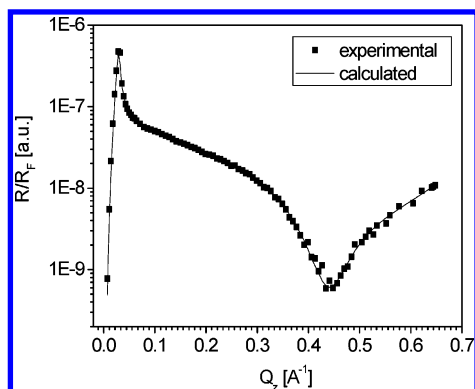


Figure 6. Fresnel-normalized X-ray reflectivity curves for the isocyanate-functionalized SAM ($t = 45$ min). Squares represent the experimental data, and the solid line, our best reflectivity fit.

conformation,³² and the thickness of the isocyanate layer was fixed at 2.5 \AA .³³

The parameters that are allowed to vary during the fit are therefore the electron densities of both the alkyl layer and the isocyanate layer, the thickness of the silicon oxide layer, the roughness of each interface, and the transition oxide parameters. The results of the modeling are shown in Table 1 (model 1), and comparison between experimental points and the adjustment is illustrated by Figure 6.

The thickness of the silicon oxide layer (11.9 \AA) is in good agreement with the value proposed by Brzoska et al. for the typical thickness of the native silicon oxide layer on a silicon substrate ($10\text{--}15 \text{ \AA}$).³⁴ The parameters obtained for the transition layer (i.e., electron density and thickness) can be attributed to a complex interface between the silicon oxide layer and TESPI molecules. The obtained electron densities calculated for the alkyl layer and the isocyanate layer lead to areas per molecule A of $24/(3.8 \times 0.312) = 20.2 \text{ \AA}^2$ and $21/(2.5 \times 0.411) = 20.4 \text{ \AA}^2$, respectively, proving the formation of a dense monolayer.²⁵

Both of these results clearly demonstrate that for a silanization time of 45 min a dense isocyanate-functionalized SAM is formed.

Chromophore Grafting. The modification of the surface energy after the grafting reaction of AB-OH molecules on the isocyanate-functionalized SAM strongly affects the water contact angle value. Indeed, we found an important increase from $53^\circ(\pm 2)$ to $69^\circ(\pm 2)$, which is in agreement with the introduction of phenyl groups onto the surface.³⁵

The grafting is evidenced by X-ray reflectivity patterns shown in Figure 7. The difference between the reflectivity curves before and after the AB-OH treatment is very important because the first minimum initially located at $Q_{\text{zmin}} = 0.434 \text{ \AA}^{-1}$ moves toward the value of $Q_{\text{zmin}} = 0.150 \text{ \AA}^{-1}$, indicating an increase in the total thickness of the film from 7.2 to 20.9 \AA as straightforwardly deduced from the relation $L = \pi/Q_{\text{zmin}}$.²⁹ The quality of the profile proves the grafting of a uniform layer onto the isocyanate-functionalized surface.

The characteristics of the film are determined by refinement (Table 1, model 2), taking into account the

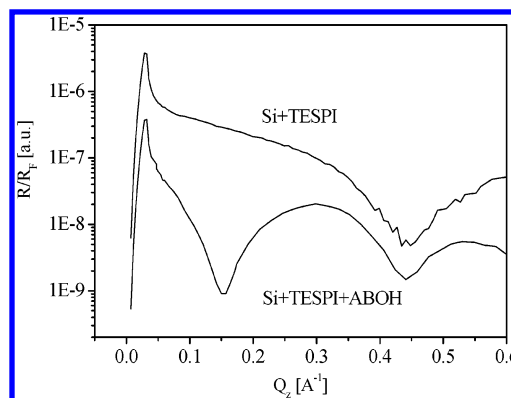


Figure 7. Fresnel-normalized X-ray reflectivity curves of the isocyanate-functionalized SAM before and after the grafting of azobenzene moieties.

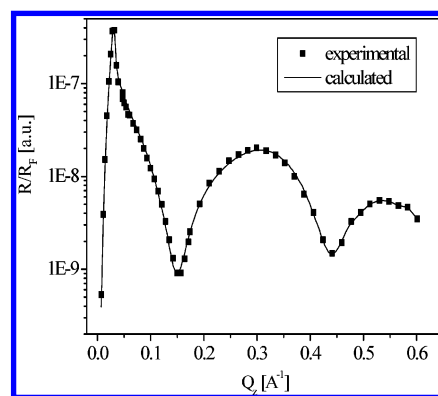


Figure 8. Fresnel-normalized X-ray reflectivity curves of the isocyanate-functionalized SAM grafted by AB-OH molecules. Squares represent the experimental data, and the solid line, our best reflectivity fit.

results obtained on the functionalized substrate (model 1). All of these parameters were fixed, and a new layer corresponding to the AB-OH molecules was added. The parameters for this layer were allowed to vary during the fit. Figure 8 illustrates the good agreement between the model and the experimental data. The thickness of the AB-OH layer was calculated to be 13.7 \AA , whereas the length of the full extended AB-OH molecule in the trans configuration was estimated to be 14.2 \AA by geometric modeling. This result can be interpreted by assuming that AB-OH molecules form a monolayer oriented with a tilt angle of 16° . The electronic density of the AB-OH layer was calculated to be $0.380 \text{ e}^- \cdot \text{\AA}^{-3}$, indicating that the layer is compact because the area per AB-OH molecule can be estimated to be 22 \AA^2 . All of these experiments clearly indicate that a dense monolayer of azobenzene derivatives is formed on the silicon surface.

Photoisomerization of the Chromophore. To estimate the parameters controlling the photoisomerization of the functionalized substrate, a spectroscopic study of the AB-OH molecules was performed. Figure 9 shows the UV-visible absorption spectra of the AB-OH solution in toluene as a function of various experimental treatments. The spectrum of a sample free from any treatment exhibits a low-intensity $n \rightarrow \pi^*$ band in the visible region ($\lambda_{\text{max}} = 443 \text{ nm}$) and a high-intensity $\pi \rightarrow \pi^*$ band in the UV ($\lambda_{\text{max}} = 327 \text{ nm}$) as previously reported for an azobenzene-type molecule.¹⁰

Irradiation of the solution for 30 s by 325 nm radiation from a He-Cd laser leads to an important decrease in the band intensity at 327 nm and an increase in the intensity of the band at 443 nm. We also note the presence of an

(32) Kuhl, T. L.; Majewski, J.; Wong, J. Y.; Steinberg, S.; Leckband, D. E.; Israelachvili, J. N.; Smith, G. S. *Biophys. J.* **1998**, *75*, 2352–2362.

(33) Gordon, A.; Ford, R. *The Chemist's Companion*; John Wiley and Sons: New York, 1972.

(34) Brzoska, J. B.; Ben Azouz, I.; Rondelez, F. *Langmuir* **1994**, *10*, 4367–4373.

(35) Moineau, J.; Granier, M.; Lanneau, G. F. *Langmuir* **2003**, *20*, 3202–3207.

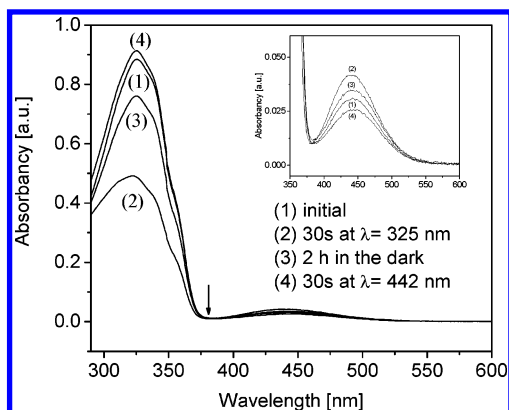


Figure 9. UV-visible absorption spectra of an AB-OH solution in toluene: (1) the initial solution, (2) after 30 s of irradiation by the He-Cd laser at $\lambda = 325$ nm, followed by (3) 2 h in the dark, and (4) by 30 s of irradiation by the He-Cd laser at $\lambda = 442$ nm.

isosbestic point at 380 nm, indicating that the modification of the spectrum is due to the *trans* \rightarrow *cis* isomerization of the AB-OH molecules.¹⁰ The initial spectrum is not fully recovered when the solution is kept in the dark for 2 h. Such a result demonstrates that the thermal back reaction is quite slow and that the molecular state of the film can be considered to be frozen during contact angle and reflectivity experiments. However, a fast recovery of the initial spectrum is observed when the sample is subjected for 30 s to the $\lambda = 442$ nm radiation of a HeCd laser at $P = 0.86 \text{ W}\cdot\text{cm}^{-2}$. Such full reversibility is attributed to the *cis* \rightarrow *trans* photoisomerization of the AB-OH molecules.

Photocontrol of the Wettability. The above investigations provide evidence of the experimental conditions allowing efficient photoisomerization of the AB-OH molecules and therefore photocontrol of the wettability of the surface.

The evolution of the water contact angle on the surface of the functionalized SAM grafted by AB-OH molecules was monitored as a function of the irradiation wavelengths. Initially, the water contact angle is equal to $69^\circ(\pm 2)$, and irradiation at 325 nm ($P = 0.33 \text{ W}\cdot\text{cm}^{-2}$) leads to a decrease in the water contact angle to $62^\circ(\pm 2)$ attributed to the *trans* \rightarrow *cis* isomerization of AB-OH molecules. Indeed, the dipole moment of the *cis* isomer is higher than that of the *trans* isomer,¹¹ which explains why *trans* \rightarrow *cis* isomerization leads to a decrease in the water contact angle. Photocontrol reversibility was demonstrated by keeping the sample in the dark for 24 h because the water contact angle recovers its initial value (69°). Photoswitching reversibility was also demonstrated by irradiating alternatively, in the visible and in the UV, a drop of olive oil on the surface of the functionalized SAM grafted by AB-OH molecules. As reported by Ischimura,⁴ oil can be used as a test liquid to prevent evaporation during irradiation experiments. Figure 10 shows the evolution of the oil contact angle measured on the functionalized SAM grafted by AB-OH molecules as a

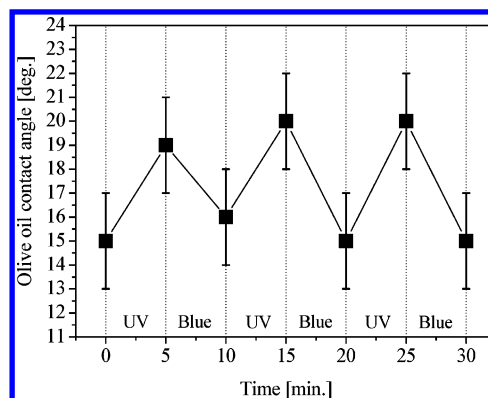


Figure 10. Evolution of the olive oil contact angle of the functionalized SAM grafted by AB-OH molecules as a function of irradiation. The columns labeled UV and Blue refer, respectively, to the sample after UV (325 nm) and blue (442 nm) light irradiation by the He-Cd laser.

function of irradiation. The oil contact angle initially equal to $15^\circ(\pm 2)$ reached $19^\circ(\pm 2)$ after 5 min exposure to 325 nm radiation at $P = 0.86 \text{ W}\cdot\text{cm}^{-2}$. Then, an irradiation of the film in the visible region contributes to the recovering of the initial contact angle value. The observed difference in the wetting behavior is attributed to the presence of two different isomers on the surface. The reproducibility was thus shown by alternating UV and visible irradiation for five cycles and by observing the periodic variation of the contact angle.

Conclusions

We have synthesized a new azobenzene molecule in order to prepare an azobenzene-containing monolayer on a silicon surface by a synthetic method consisting of the covalent grafting of azobenzene derivatives onto an isocyanate-functionalized SAM. Characterization of the isocyanate-functionalized SAM by contact angle measurement, X-ray reflectivity, and AFM demonstrates that the procedure used to graft azobenzene molecules onto the isocyanate-functionalized SAM has permitted us to obtain a dense azobenzene monolayer. In solution, we have shown that our synthesized azobenzene was able to switch between two different steady states after having been irradiated for 30 s with the two available wavelengths of a HeCd laser ($\lambda = 325$ and 442 nm). Photoswitching of the wettability of the functionalized SAM grafted by AB-OH molecules was then demonstrated with water and oil. Even though the variation of the water contact angle ($\Delta\theta = 7^\circ(\pm 2)$) could be considered to be modest, Aoki et al. have shown that this variation is enough to control the large-scale alignment of a liquid crystal.¹⁷

Acknowledgment. This work was supported by the French PIR "Microfluidique et Microsystèmes Fluidiques 2003" under project MI2F03-44. We thank S. Lesko from Veeco for providing the AFM image.

LA051517X